Synthetic Metals 158 (2008) 1062–1066

Contents lists available at ScienceDirect

Synthetic Metals

journal homepage: www.elsevier.com/locate/synmet

Letter

Singlet to triplet excitation spectrum of thin film tris-(8-hydroxyquinolate)-aluminium in direct absorption

ARTICLE INFO

Keywords:
OLED
Triplet
Absorption
Tris-(8-hydroxyquinolate)-aluminium
Cavity ringdown
Spectroscopy

ABSTRACT

We report the excitation spectrum of a ~185 nm thick layer tris-(8-hydroxyquinolate)-aluminium, vapour deposited on a 100 μm thick borosilicate microscopy cover glass, in the 1.9–2.4 eV range using a conventional cavity-ringdown spectrometer setup. The spectrum is collected at room temperature in an open cavity. It shows a broad loss structure with a maximum around 2.1 eV and a width of ~0.2 eV. The spectrum is in conformity with literature phosphorescence spectra and with literature TDDFT computed $T_1 \leftarrow S_0$ transition energies. The observed loss structure can be attributed to the $T_1 \leftarrow S_0$ absorption band of tris-(8-hydroxyquinolate)-aluminium.

1. Introduction

Tris-(8-hydroxyquinolate)-aluminium (AlQ_3) is a frequently applied material in the field of organic light-emitting diodes (OLEDs), either as an emitting material, or as non-emitting material such as electron-transporter or matrix or host material. AlQ_3 has become one of the best characterized OLED materials in the last decades.

In OLEDs AlQ_3 essentially acts as a singlet emitter. Unfortunately, there is a preference for populating the triplet states when electrically exciting an OLED. This preference is basically driven by entropy: the probability of populating a triplet state is a factor three higher than for a singlet state of the same energy, due to the threefold degeneracy of the triplet state. Furthermore, there is in general also an energy drive: the lowest excited triplet state is normally lower in energy than the lowest excited singlet state, thus, the occupation probability increases to above 0.75. This preferred population of triplet states reduces the quantum efficiency of OLEDs when using essentially fluorescent materials. Knowledge about the triplet bands both of emitting and of non-emitting OLED materials is of crucial importance for a good understanding of the spectral and transport properties of these materials so that their triplet states can be exploited better in the design of devices with a higher quantum efficiency.

Many properties of AlQ_3 have been reported [1–3] as a result of computer simulations. Among them there are the singlet ← singlet (S ←S) and triplet ← singlet (T ←S) transitions which compare well to available S ← S absorption spectra and to (prompt and delayed) fluorescence and phosphorescence spectra [4,5]. However, the AlQ_3T ← S spectrum is difficult to record due to the spin-forbidden transition involved, resulting in a small absorption cross-section. To date, there are absorption spectroscopic methods available that have the potential of detecting such weak transitions. Among them there is cavity ringdown spectroscopy (CRDS).

In 1988 CRDS was first applied to record weak absorption lines from the triplet groundstate of gas-phase molecular oxygen to its first excited singlet state [6]. Since then, CRDS has become an established spectroscopic method for recording weak absorption features or for exploiting strong absorption features in samples with a low absolute number-density of absorbers [7,8](and references therein). Furthermore, CRDS is not limited to absorbing species, or to species in the gas-phase, only. Also a number of experiments on CRDS applied to liquids [9–11], or to thin films [12–18] have been reported, moreover, other weak spectroscopy features, such as polarization rotation of light due to a magnetic field [19,20] and *e.g.*, Rayleigh scattering cross-sections of Ar, N_2, and SF_6, have been determined accurately [21].

Complementary to standard double-beam absorption spectrometers, which can be sensitive in absorbance down to the $\alpha \sim 10^{-3}$ to 10^{-5}range, CRDS is best suited for the range of absorbances of $\alpha = 10^{-4}$ down to around 10^{-7} to 10^{-8}. Here the absorbance $\alpha = \kappa d$ is the dimensionless product of the absorption coefficient κ and the path length d through the absorbing species.

In a CRDS experiment a stable cavity with a high quality-factor is used. The most frequently used type of ringdown cavity consists of two equivalent highly reflective mirrors, face to face, with reflectivities of usually $R > 0.999$. Other types of cavities, exploiting total internal reflection, have been applied successfully too, such as small sub-cm sized prisms [22–24], a μm sized toroidal cavity [25], and a glass fiber cavity [26].

Considering a traditional two-mirror cavity, light coupled into this cavity via the – normally not highly reflective – backside of one of the mirrors, is captured in the cavity and a cavity field is built up. The intensity I of this field at a certain time depends on the number of photons N stored in the cavity while the change in intensity depends on the net number of photons lost from the cavity per unit of time. This parameter is a function of several intra-cavity light-loss-terms with the most important being: (1) non-total reflection of the mirror surfaces, (2) absorption due to species in the cavity, (3) diffraction due to structures in the cavity (including the mirrors, *i.e.*, excitation of TEM modes), (4) scattering at the sample and at other species and imperfections in the cavity. The order of importance of these terms is more or less arbitrary and may vary for different experimental configurations. In any case, for a known intensity-

0379-6779/$ – see front matter © 2008 Elsevier B.V. All rights reserved.
doi:10.1016/j.synthmet.2008.02.015

profile as a function of time of the incoupled light, any of the above mentioned terms can be determined provided that a change in that one term is not correlated to changes in one of the other terms. In particular, for an absorption measurement when using a short duration input light pulse the time dependent intensity of the cavity-field follows, under restrictions [27], an exponential decay: $I(t) \sim \exp(-t/\tau)$ with time-constant the *ringdown time* $\tau = l/c \times \mathcal{L}^{-1}$. Here l is the mirror separation, c is the velocity of light in the cavity medium, and $\mathcal{L} = \mathcal{L}_{\text{refl}} + \mathcal{L}_{\text{abs}} + \mathcal{L}_{\text{diffr}} + \mathcal{L}_{\text{scat}} + \cdots$ is the sum of all the cavity-loss-terms. In this case, $\mathcal{L}_{\text{abs}}(= \kappa d = \alpha)$ can be extracted from the ringdown times of two measurements: one with and one without the absorbing species present, via: $\mathcal{L}_{\text{abs}} = l/c \times [(\tau_{\text{with}})^{-1} - (\tau_{\text{without}})^{-1}]$, provided that $(\mathcal{L} - \mathcal{L}_{\text{abs}})$ is uncorrelated with $\mathcal{L}_{\text{abs}}$.

2. Experimental

A sample is prepared by mounting a 25 mm × 25 mm ×100 μm sized non-fluorescent borosilicate microscopy cover glass in a vacuum tank with one side facing an evaporation source. Half of this side is covered with aluminium foil to prevent layer deposition. With AlQ_3 powder placed in the evaporation source and heated to a temperature of ∼600 K a deposition rate of $\sim 3 \times 10^{-2}$ nm/s is maintained for 1.5 h at a chamber pressure of $\sim 10^{-6}$ Torr. The deposition rate is obtained from the frequency change due to deposition of AlQ_3 onto a vibrating calibration crystal that is simultaneously exposed to the evaporation source. Later on profilometry on scratches in the AlQ_3 layer, at different locations of the sample and after the cavity ringdown experiments have finished, indicates a thickness of 185 ± 28 nm. The foil-covered half of the substrate remains blank such that, later on, a data point with and without the AlQ_3 layer present can be collected from the same substrate without damaging the AlQ_3 layer. In Fig. 1 (inset) the layout of the substrate is depicted.

A cavity ringdown spectrometer is configured by combining a Spectra Physics Quanta-Ray GCR series Nd^+:YAG laser pumped OPO (Spectra Physics MOPO; pulse duration ∼3 ns; bandwidth ∼0.3 cm^{-1}) with a two mirror ringdown cavity (mirrors: Los Gatos Research Inc.; $R_{580\,\text{nm}} > .99995$, $R_{(555\,\text{nm},605\,\text{nm})} > .99990$, $r = 1$ m (r: radius of curvature)), a photo-multiplier tube (PMT) (Hamamatsu), and a digital oscilloscope (LeCroy; 1 GHz, 5 GS/s, 8 bit vertical resolution). A scheme of the setup used is shown in Fig. 1. Before fed into the ringdown cavity the signal of the MOPO is tightened and skimmed by a factor ∼ 3 via a telescope with an iris (∼.5 mm) near the focal point. Together with additional irises in front of the first focusing lens (∼5 mm) and in front of the cavity mirror (∼.5 mm) these optics serve the purpose of alignment and beam shaping. The cavity itself is set up as an open cavity, *i.e.*, mirrors and sample holder are placed on a breadboard in ambient atmosphere. This provides easy access to the sample holder for (1) adjustment of the mirrors and the sample and (2) interchange of the substrate with AlQ_3 layer with a blank substrate for a background correction measurement.

With the sample holder mounted on a manually activated linear stage, in between two mirrors that form the ringdown cavity of $l = 20$ cm length, it becomes possible to move the substrate perpendicularly, and with a high reproducibility, through the cavity with respect to the optical axis. Thus, the cavity stability is consolidated when subjecting different areas of the substrate to the cavity field. Placement of the substrate with its normal parallel to the optical axis and equidistantly between the two cavity mirrors provides an irradiation spot size on the order of the beam waist dimension, computed via [28]: $w_0 = (\lambda/n\pi)^{1/2} \times (l/2 \times (r - l/2))^{1/4} \sim 0.3$ mm in the TEM_{00} mode, at the maximum wavelength generated by the MOPO of $\lambda \sim 650$ nm. The refractive index n of the cavity medium is taken unity. This indicates that the available area of ca. 14.6 mm diameter on both halfs of the substrate is sufficient to either irradiate the AlQ_3 covered half of the sample, or its blank half. The instability introduced by the two parallel reflecting surfaces of the substrate, forming an essentially unstable subcavity, is negligible due to the low reflectivity of both surfaces and due to its small thickness with respect to the main cavity length. CRDS experiments by others have proven this a reliable cavity configuration in the past [12,17].

An alternative substrate orientation reported in literature [9,10,14,15,18], where the sample is placed under the Brewster angle, is unfavourable in this experiment due to the substantially higher refractive index of AlQ_3($n = \epsilon^{1/2} \sim 1.7$ computed [29] from

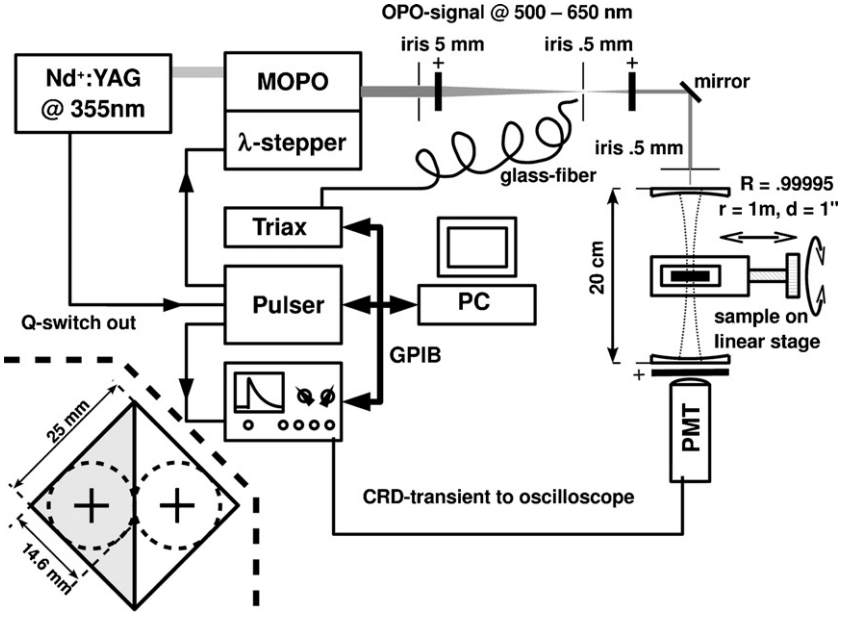

Fig. 1. Main figure: schematic of the CRD spectrometer setup used. Inset lower left: layout of the borosilicate glass substrate with one half blank and the other half covered with AlQ_3. Indicated are the areas on both halfs available for irradiation.

its dielectric constant $\epsilon = 3.0 \pm 0.3$ reported in, *e.g.*, Ref. [3]) with respect to that of borosilicate glass ($n \sim 1.5$). Thus, (1) there is a different Brewster angle for both faces of the sample, causing an unwanted – and likely too high for CRDS – cavity-loss due to reflection at the sample, and (2) it introduces the necessity of separate adjustments of the sample for a recording with AlQ_3 present and for a recording of the blank substrate. Both items will cause extra uncertainty in the interpretation of the intensities of the spectrum to be obtained.

Via a glass fiber, light, scattered at one of the optical elements in the MOPO-signal-beam path, is guided into a grating spectrometer (Horiba-Jobin-Yvon Triax) serving wavelength calibration. To trigger the experiment the Q-switch of the Nd^+:YAG provides the source-trigger which is directed via a pulser/delay generator (Highland Technology) to the oscilloscope and the MOPO. The MOPO wavelength stepper lacks control-ports (*e.g.*, RS232, GPIB, RJ45) and cannot be stepped remotely via a personal computer (PC). However, the pulser can be remotely controlled and allows for MOPO-control via temporarily switching the MOPO's trigger line to a continuous 5 V, thereby preventing the stepper from counting trigger-pulses and stepping unwantedly to a new wavelength, while the oscilloscope data is processed and stored on the PC and the instruments are prepared for collecting a data point at a new wavelength.

The PC, running National Instruments LabView 7.0, controls the experiment via GPIB connections to the pulser, the oscilloscope, and the grating spectrometer. The light transmitted through one of the cavity mirrors is collected with the PMT via a focusing lenses, and converted into an electric voltage transient which is read and processed by the oscilloscope. The high voltage supply of the PMT is manually adjusted when necessary, while scanning the MOPO over a certain wavelength range, such that the vertical resolution of the oscilloscope is optimally exploited. Per wavelength step, ringdown transients are collected and averaged by the internal arithmetic functions of the oscilloscope. The averaged trace is submitted to the PC where the cavity loss spectrum is deduced.

A measurement session consists of two scans: the first scan runs over the wavelength range using the sample with AlQ_3, followed by a second scan over the same wavelength range using the blank substrate. No adjustment of mirrors and/or substrate takes place between this pair of scans. The scan-order is important to be confident that a measured difference in the ringdown time with the AlQ_3 layer and without this layer can be attributed to the presence of this layer and is not due to an altered alignment after moving the sample via the linear stage, *i.e.*, in the current scan sequence the ringdown times *increase* in the second scan with respect to those in the first scan, which is not likely to happen due to an accidentally altered cavity alignment after this has been optimized already shortly before the session commenced. Data points are collected at equidistant intervals of 5 nm from 500 through 700 nm MOPO setting which – non-linearly – projects to 500 through 650 nm measured wavelength with the grating spectrometer. Averaging over 500 shots per data point at a repetition rate of 10 Hz yields both appreciable signal to noise ratio and scan-duration. During each measurement session the cavity and PMT are covered with a synthetic lightproof and dust free sheet. This sheet allows for manual adjustment of the mirrors and the sample before the session starts meanwhile preventing background light from exciting the PMT.

3. Results and discussion

In the CRDS setup used the ringdown time at the mirror-optimum of 580 nm was maximum $\tau_{empty} = 6.3\mu$ s for a

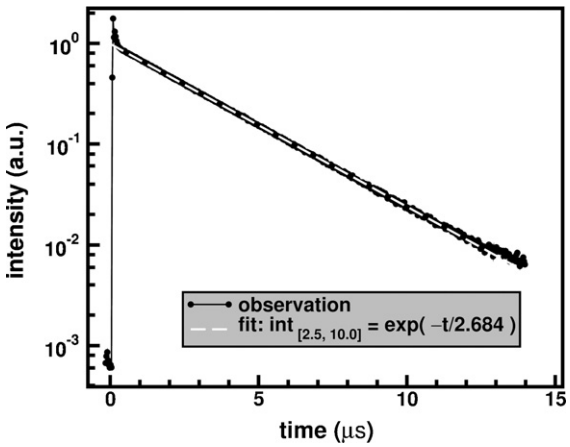

Fig. 2. Ringdown transient on a semi-log scale observed for 2.1 eV excitation energy of the cavity with the blank borosilicate glass substrate present. A least squares fit to the datapoints between 2.5 and 10 μs yields a ringdown time of $\tau = 2.684\mu$s.

furthermore empty cavity. Ideally, with a reflectivity of $R > .99995$, for an empty cavity of $l = 20$ cm the maximum obtainable ringdown time should be $\tau_{th} > l \times [c(1-R)]^{-1} = 13.3\mu$s. The reduction with a factor of two in our setup is probably due to an in fact non-empty cavity. In the open cavity used, air is the carrier of many microscopical sized dust particles, water droplets, etc. which cause non-resonant scattering losses and limit the maximum obtainable ringdown time. With the clean borosilicate glass substrate in the cavity the ringdown time reduces approximately by another factor two. An example of a ringdown transient for the substrate, together with a least squares fit, and recorded at 2.1 eV (≙590 nm) excitation energy, is presented on a semi-log scale in Fig. 2. The ringdown time of 2.684 μs indicates an effective reflectivity with the substrate present of $R_{eff} = .99975$ which means a reduction with a factor five in detection limit [27] compared to the ideal cavity without substrate.

In Fig. 3 the cavity-loss spectra of the AlQ_3 coated and the uncoated half of the borosilicate glass substrate are presented as a function of the excitation energy. From the cavity loss of Fig. 3 the AlQ_3 contribution to the cavity-loss follows from subtraction of the two traces and is presented in Fig. 4. Assuming the absorption losses being the only remaining losses after subtraction, and uncorrelated

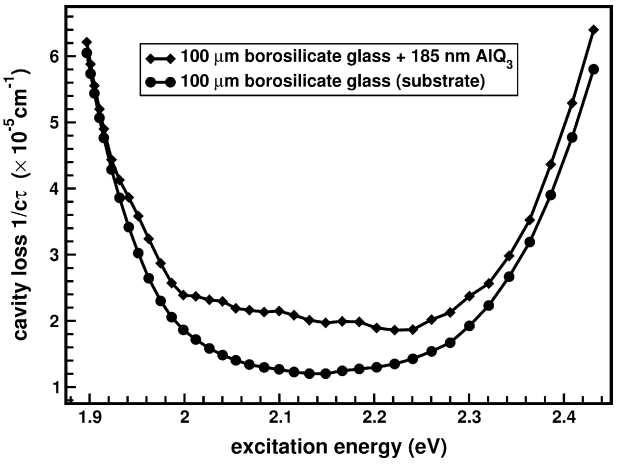

Fig. 3. Cavity loss spectra of the ringdown cavity with blank substrate (disks) and with AlQ_3 covered substrate (diamonds) as a function of the excitation energy. The overall loss structure is due to the varying mirror reflectivity over the energy scan-range applied.

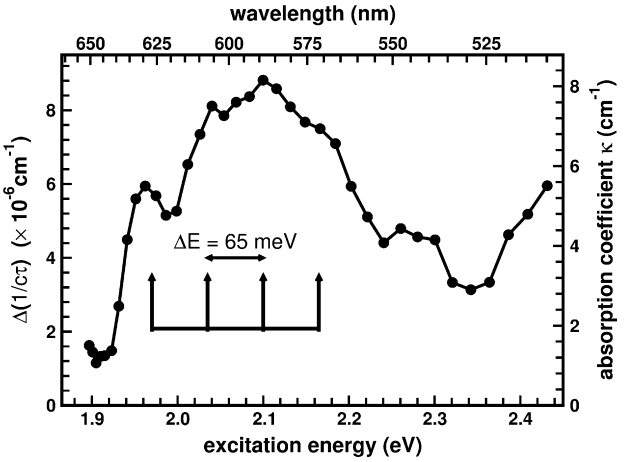

Fig. 4. Difference spectrum of the two traces of Fig. 3, representing the AlQ_3 related cavity loss as a function of the excitation energy. On the right axis is the equivalent absorption coefficient for AlQ_3 indicated, provided that no other losses have contributed to the spectrum but absorption losses. On the top the wavelength equivalent for the excitation energy is indicated. The comb inside the graph marks a regularly spaced substructure that could be originating from a vibrational progression.

with other losses, the absorption coefficient linearly depends on the difference of both cavity-loss spectra via $\kappa = \Delta[c\tau]^{-1} \times ld^{-1}$ and is indicated on the right axis of the graph. A broad spectral structure is observed with a maximum at 2.1 eV and a width of roughly 0.2 eV at half height. On the high energy part there is an increase of the cavity loss with increasing excitation energy. Although the signal to noise ratio and spectral data point sampling are not good enough for an unambiguous assignment, there seems to appear a regularly spaced structure, indicated in the figure with a comb, with a spacing of $\sim 0.065 \pm 0.005$ eV ($\hat{=}525 \pm 40\,\mathrm{cm}^{-1}$).

Time-dependent density functional theory (TDDFT) computed optical transitions of AlQ_3 have been reported [3] with the components of the lowest triplet state at 2.13, 2.16, and 2.19 eV from the electronic groundstate, while the second lowest triplet state is computed at 2.79 eV slightly above the first excited singlet state (2.77 eV). Furthermore, the dominant transitions of the S ← S absorption spectrum are the 2nd and the 4th singlet states slightly below 3 eV. These computed excitation energies compare well with the literature observed absorption spectra of AlQ_3 in dense thin-films [3,30,31], that show a weak tail from ~2.3 to 2.7 eV and a steep onset to a maximum around 3.1 eV.

The spectrum presented in Fig. 4 is in conformity with these computed and observed results published, if the broad absorption is due to T ← S excitation. In this case the observed increase in absorption in the region above 2.3 eV can be attributed to excitation of the mentioned weak tail in the S ← S absorption spectrum. This tail may be due to transitions from vibrationally excited states in the groundstate to the excited singlet and triplet states computed around 2.75–2.8 eV. Emission (phosphorescence) spectra of AlQ_3 from ~2.06 eV (600 nm) with a maximum down at 1.77 eV (700 nm) have been recorded [4,5] via electro-luminescence. In these emission spectra a vibrational progression is identified with a spacing of ~0.07 eV (or 560 cm^{-1}) which has been attributed to an earlier reported vibrational mode [32,33] of AlQ_3. In the CRD spectrum presented here, the majority of absorption observed is above 2.06 eV with a small overlap region. This conforms with the phosphorescence spectra reported in literature and reflects a normal Stokes shifted emission band with respect to the absorption. Furthermore, the indication of a progression in the CRD spectrum of a spacing slightly smaller than is observed in the phosphorescence spectrum, supports that the transition is essentially between two electronic bands: in the phosphorescence spectrum the vibrational progression in the electronic groundstate is revealed, whereas, in the absorption spectrum that of the equivalent vibration in the electronically excited state is revealed. This latter usually has a slightly smaller spacing [34].

Phosphorescence lifetimes for AlQ_3 have been reported for 30, 50, and 80 K, and yield 8.1 (9.1), 7.0, and 5.6 (5.9) ± 0.5 ms [4](bracketed values for Ref. [5]), respectively. Via the relation between the natural lifetime and the absorption coefficient $\kappa(\nu)$ [34] a lifetime estimate (in μs) can be computed via: $\tau_{\mathrm{rad}} = 2.53 \times 10^3 \times g_2 g_1^{-1} N \nu_0^{-2} [\int \kappa(\nu)\,\mathrm{d}\nu]^{-1}$, when expressing N in nm^{-3}, ν, ν_0 in eV, and κ in cm^{-1}. Moreover, the spectrally integrated cross-section in $\mathrm{eV\,cm}^2$ yields $\int \sigma(\nu)\,\mathrm{d}\nu = 10^{-21} \times N^{-1} \int \kappa(\nu)\,\mathrm{d}\nu$. Here, the degeneracies of the groundstate (g_1) and excited state (g_2) are difficult to determine. The density of (vibrational) states must be computed for the ground- and excited electronic states so that the contributions to τ_{rad} of all possible transitions from the Boltzmann distributed electronic groundstate and per excitation energy can be accounted for appropriately. We set this ratio is to $g_2 g_1^{-1} = 3$, so that at least the threefold degeneracy of the, assumed, triplet excited state with respect to the non-degenerate singlet groundstate is included. Furthermore, the central frequency ν_0 is ill-defined in the observed asymmetric and likely inhomogeneously broadened spectrum. This frequency is set to the maximum of the most prominent band $\nu_0 = 2.1$ eV. The crystalline AlQ_3 number-density $N = 2\,\mathrm{nm}^{-3}$ is reported in literature [3] and used here, although the degree of crystallization is unknown for the sample used. The integral over the spectral range up to 2.35 eV of the observed CRD spectrum yields: $\int \kappa(\nu)\,\mathrm{d}\nu = 3\,\mathrm{eV\,cm}^{-1}$. With these values a rough indication of the natural lifetime is found of: $\tau_{\mathrm{rad}} \sim 1$ ms with a band integrated cross-section of $\int \sigma(\nu)\,\mathrm{d}\nu \sim 1.5 \times 10^{-21}\,\mathrm{eV\,cm}^2$ over a bandwidth of ~0.5 eV. If a singlet excited state was assumed the lifetime would be decreased by a factor 3 in our computation as a consequence of altering the value of $g_2 g_1^{-1}$ from 3 to 1. This lifetime is orders of magnitude longer than usual for a singlet excited state with a low principal quantum-number, whereas, its duration is not uncommon for a triplet state, and of the same order of magnitude as the reported observed lifetimes mentioned earlier. Note further that: (1) we have in fact recorded the cavity-loss spectrum. It cannot be excluded that other than absorption losses, *i.e.*, scattering of light at the AlQ_3 layer, have occurred. Their non-resonant nature may cause a monotonously increasing (with increasing excitation energy) background. (2) The density of vibrational states in the triplet state is likely higher than in the singlet state, *i.e.*, due to an expected closer spacing of the vibrational levels in the excited state, so that $g_2 g_1^{-1} > 3$, and (3) in the high energy part of the spectrum there may be overlap with the red tail of the $S_1 \leftarrow S_0$ band. These arguments favour a smaller integrated absorption coefficient $\int \kappa(\nu)\,\mathrm{d}\nu$ for the $T_1 \leftarrow S_0$ band which explains that the lifetime computed for this band is shorter than its observed lifetime. Therefore, the absorption band is identified with the $T_1 \leftarrow S_0$ absorption band of AlQ_3.

4. Conclusions

We have recorded the $T_1 \leftarrow S_0$ absorption spectrum of a 185 nm layer of AlQ_3, deposited on a borosilicate microscopy cover glass, in direct absorption via CRDS. The spectrum recorded is in conformity with its literature phosphorescence spectra, in position and in intensity. From the integrated intensity the phosphorescence lifetime is roughly estimated to be in the ms range, which is of the same order of magnitude as observed phosphorescence lifetimes for AlQ_3. CRDS can be used to determine triplet absorption bands in thin layers of organic materials. As an absorption spec-

troscopic method CRDS is not limited to emissive species alone. It could also be applied to species that show no phosphorescent spectrum and for which triplet states cannot be investigated via photo- and/or electro-luminescence, *e.g.*, hole-blockers, electron transport materials, and matrix-materials, all of which are used in organic semiconductor devices.

Acknowledgements

We gratefully acknowledge Dr. Jos Oomens of the Institute for Plasmaphysics Rijnhuizen in Nieuwegein, the Netherlands, for supporting their "MeasureIt" code, written in LabView, which we modified and used for experimental control. Furthermore we thank the skillful support of the National Nanotechnology Laboratory technical staff: Sonia Carallo and Elisabetta Perrone who helped and advised with the vapour deposition of AlQ_3, and Dr. Marco Salerno who is thanked for help and advise with the use of the profilometer.

References

[1] A. Curioni, M. Boero, W. Andreoni, Chem. Phys. Lett. 294 (1998) 263.
[2] A. Curioni, W. Andreoni, R. Treusch, F.J. Himpsel, E. Haskai, P. Seidler, C. Heske, S. Kakar, T. Van Buuren, L.J. Terminello, Appl. Phys. Lett. 72 (1998) 1575.
[3] R.L. Martin, J.D. Kress, I.H. Campbell, D.L. Smith, Phys. Rev. B 61 (2000) 15804.
[4] M. Cölle, C. Gärditz, Appl. Phys. Lett. 84 (2004) 3160.
[5] M. Cölle, C. Gärditz, A.G. Mückl, Synth. Met. 147 (2004) 97.
[6] A. O'Keefe, D.A.G. Deacon, Rev. Sci. Instrum. 59 (1988) 2544.
[7] G. Berden, R. Peeters, G. Meijer, Int. Rev. Phys. Chem. 19 (2000) 565.
[8] G. Berden, G. Meijer, W. Ubachs, Exp. Meth. Phys. Sci. 40 (2002) 47 (Chapter 2).
[9] S. Xu, G. Sha, J. Xie, Rev. Sci. Instrum. 73 (2002) 255.
[10] K.L. Snyder, R.N. Zare, Anal. Chem. 75 (2003) 3086.
[11] B. Bahnev, L. van der Sneppen, A.E. Wiskerke, F. Ariese, C. Gooijer, W. Ubachs, Anal. Chem. 77 (2005) 1188.
[12] R. Engeln, G. Von Helden, A.J.A. Van Roij, G. Meijer, J. Chem. Phys. 110 (1998) 3763.
[13] D. Kleine, J. Lauterbach, K. Kleinermanns, P. Hering, Appl. Phys. B 72 (2001) 249.
[14] G.A. Marcus, H.A. Schwettman, Appl. Opt. 41 (2002) 5167.
[15] R.N. Muir, A.J. Alexander, Phys. Chem. Chem. Phys. 5 (2003) 1279.
[16] A.C.R. Pipino, J.P.M. Hoefnagels, N. Watanabe, J. Chem. Phys. 120 (2004) 2879.
[17] I.M.P. Aarts, B. Hoex, A.H.M. Smets, R. Engeln, W.M.M. Kessels, M.C.M. Van de Sanden, Appl. Phys. Lett. 84 (2004) 3079.
[18] J. Antonietti, M. Michalski, U. Heiz, H. Jones, K.H. Lim, N. Rörsch, A. Del Vitto, G. Pacchioni, Phys. Rev. Lett. 94 (2005) 213402.
[19] R. Engeln, G. Berden, E. Van den Berg, G. Meijer, J. Chem. Phys. 107 (1997) 4458.
[20] G. Berden, R. Engeln, P.C.M. Christianen, J.C. Maan, G. Meijer, Phys. Rev. A 58 (1998) 3114.
[21] H. Naus, W. Ubachs, Opt. Lett. 25 (2000) 347.
[22] A.C.R. Pipino, J.W. Hudgens, R.E. Huie, Chem. Phys. Lett. 280 (1997) 104.
[23] A.C.R. Pipino, Phys. Rev. Lett. 83 (1999) 3093.
[24] A.C.R. Pipino, Appl. Opt. 39 (2000) 1449.
[25] D.K. Armani, T.J. Kippenberg, S.M. Spillane, K.J. Vahala, Nature 421 (2003) 925.
[26] R.S. Brown, I. Kozin, J. Chem. Phys. 117 (2002) 10444.
[27] P. Zalicki, R.N. Zare, J. Chem. Phys. 102 (1995) 2708.
[28] A. Yariv, Quantum Electronics, third edition, ISBN 0-471-61771-7, 1988.
[29] J.D. Jackson, Classical Electrodynamics, second edition, ISBN 0-471-43132-X, 1975.
[30] T. Mori, H. Tsuge, T. Mizutani, J. Phys. D: Appl. Phys. 31 (1999) L65.
[31] V.A.L. Roy, R.B. Pode, Thin Solid Films 417 (2002) 180.
[32] M. Braun, J. Gmeiner, M. Tzolov, M. Cölle, M. Meyer, W. Milius, H. Hillebrecht, O. Wendland, J. Von Schütz, W. Brütting, J. Chem. Phys. 114 (2001) 9625.
[33] M. Brinkmann, G. Gadret, G. Muccini, C. Taliani, N. Masciocchi, A. Sironi, J. Am. Chem. Soc. 122 (2000) 144.
[34] J.I. Steinfeld, Molecules and Radiation—An Introduction to Modern Molecular Spectroscopy, ISBN 0-262-69059-4, 1978.

J.A. (Hans) Piest*
Universität Duisburg-Essen, Fakultät für Ingenieurwissenschaften, IVG Nanopartikel-Prozesstechnik, Lotharstraße 1, 47057 Duisburg, Germany

M. Anni
R. Cingolani
G. Gigli
National Nanotechnology Laboratory, 73100 Lecce, Italy

* Corresponding author. Tel.: +49 203 379 2511; fax: +49 203 379 4453.
E-mail addresses: hans.piest@uni-due.de, hans.piest@gmx.de (J.A. (Hans) Piest)

3 December 2007

Available online 18 April 2008